Functional properties of soybean nodulin 26 from a comparative three-dimensional model

Sampa Biswas*

Crystallography and Molecular Biology Division, Saha Institute of Nuclear Physics, 1/AF Bidhannagar, Kolkata 700 064, India

Received 6 November 2003; revised 12 December 2003; accepted 18 December 2003

First published online 12 January 2004

Edited by Robert B. Russell

Abstract A model of the nodulin 26 channel protein has been constructed based on comparative modeling and molecular dynamics simulations. Structural features of the protein indicate a selectivity filter that differs from those of the known structures of *Escherichia coli* glycerol facilitator and mammalian aquaporin 1. The model structure also reveals important roles of Ser207 and Phe96 in ligand binding and transport.

Key words: Nodulin-like intrinsic protein; Comparative model; Transmembrane helix; Selectivity filter; Formamide

1. Introduction

Aquaporins (AQPs) are an ancient family of channel proteins that transport water and non-ionic small metabolites across the biological membranes. Structure of these proteins enforces high specificity for a particular solute when allowing high flux of the solute. AQPs are members of the major intrinsic protein (MIP) family, a widespread membrane channel proteins that has been identified in bacteria, fungi, insects, plants and animals having more than 200 members [1,2]. Based on their function, they have been classified into three major subgroups: (1) AQPs (AQP family), specific for water transport; (2) glycerol facilitator (GlpF family), transporting small linear carbohydrates like glycerol, ribitol, xylitol, etc. and (3) aquaglyceroporin (AQP3 family), transporting water, glycerol and small non-ionic solutes [2].

In plants, AQPs are present in tonoplast, plasma membrane and in other internal membranes like the symbiosome membrane (SM) of symbiotic nitrogen fixing bacteria at infected root nodules [3,4]. About 30 genes are present in the *Arabidopsis* genome [5] and 31 are present in *Zea mays* [6]. This family of genes in plants can be divided into four phylogenetic subfamilies – the tonoplast intrinsic proteins (TIPs), the plasma membrane intrinsic proteins (PIPs), the nodulin-like intrinsic proteins (NIPs) and the small basic intrinsic proteins (SIPs) [7]. The phylogenetic classification has good agreement with the subcellular localization and function of these subclasses. The function and intracellular localization of SIPs are yet to be addressed.

The AQP family arose from gene duplication and the N-terminal segment has ~20% conservation with the C-terminal segments [8]. Both the segments contain a highly conserved –NPA– (–Asn–Pro–Ala–) motif. High resolution structures of AQP1 from bovine red blood cells [9] and GlpF from *Escherichia coli* [10] determined by the X-ray crystallographic method, reveal a homotetrameric form of the protein with similar overall transmembrane helices and monomer association. In both the cases, monomers are related by a four-fold axis and each monomer, containing six tilted membrane-spanning helices and two half membrane-spanning helices surrounding a central channel, forms an hourglass model [2] with the narrowest constriction at the middle of the channel. This constriction region contains the characteristic –NPA– motif from both the segments, common to all AQPs [9,10]. Structural and molecular dynamics studies [11–15] indicate the presence of a high-affinity binding site near the outlet at the extracellular site of the channel in AQPs, the appropriate electrostatic environment and the size complementary of which are to some extent responsible for the selective binding and subsequent transport of specific solute(s) through the channel. This region is called the selectivity filter [12].

Plant PIPs and TIPs cluster together with animal AQPs according to a phylogenetic study [16] but NIPs form a different group. Nodulin 26, a member of the NIP family, is found in soybean (*Glycine max*) root nodule SM when infected by *Bradyrhizobium japonicum*. It transports water, glycerol, formamide, malate, etc., with highest permeability towards formamide, from host to bacteria to meet the bacteria's metabolite requirements [17]. There is at least one reference where a possibility of transporting ammonia as an uncharged solute through this protein has been mentioned [18]. Nodulin 26 is the major protein component of the soybean SM and is a target of phosphorylation which regulates its water and solute transport rate [19]. A recent study [20] suggests CpNIP1 from zucchini, a member of NIP family can transport urea. Detailed knowledge of the structure of this class of proteins is required to understand this broad selectivity.

The extent of sequence identity of AQP1 from the mammalian system and GlpF from *E. coli* with NIP family proteins and structural homology in the conserved transmembrane helices among the known structures suggested a feasibility of comparative protein structure modeling of nodulin 26,

*Fax: (91)-33-2337 4637.
E-mail address: sampa@cmb2.saha.ernet.in (S. Biswas).

Abbreviations: AQP, aquaporin; GlpF, glycerol facilitator; SM, symbiosome membrane; NIP, nodulin-like intrinsic protein; TIP, tonoplast intrinsic protein; SIP, small basic intrinsic protein; POPE, palmitoyloleyl phosphatidyl-ethanolamine; –NPA–, –Asn–Pro–Ala–

0014-5793/04/$30.00 © 2004 Published by Elsevier B.V. on behalf of the Federation of European Biochemical Societies.
doi:10.1016/S0014-5793(03)01529-1

the best biochemically characterized [17–19,21,22] protein in the NIP family. Here we report a homology model of the tetramer unit of nodulin 26 with two formamide molecules docked in the channel of each monomer in the membrane environment.

Structural studies based on the homology model of nodulin 26 reveal a selectivity filter and a ligand binding pattern which is different from AQP1 and GlpF. The model structure supports the phylogenetic classification that NIPs form a separate subfamily of AQPs based on amino acid sequence.

2. Materials and methods

2.1. Sequence analysis

Multiple sequence alignment by CLUSTAL W (http://www.ebi.ac.uk/clustalw) was used to compare the sequence of nodulin 26 with the representatives of AQP subfamilies like AQPs, AQP3 and NIP (Fig. 1).

2.2. Comparative modeling of monomeric nodulin 26

The protein sequence of nodulin 26 (acc. no. P08995) was submitted to the SWISS-MODEL server (Automated Comparative Protein Modeling Server, Version 3.5, GlaxoWellcome Experimental Research, Geneva, Switzerland) [23] for comparative protein structure modeling. Structures having more than 25% sequence identity with the target sequence (nodulin 26) were selected initially by the program from the template library ExPDB extracted from the PDB database [24]. A structural alignment was performed among these structures to identify the core region of the selected structures and the top five structures with low Cα root mean square (rms) deviation values for the core region were selected as templates. Templates selected in this way were bovine AQP1 (PDB code: 1j4n), human AQP1 (PDB code: 1fgy, 1ih5, 1h6i) and *E. coli* GlpF (PDB code: 1fx8). A previous study [12] on these five structures also shows a close resemblance in their transmembrane helical region as indicated by low rms deviation values (0.9–2.67 Å for helix backbone atoms) between the structural pairs using these structures. This observation also added confidence for selecting these structures as templates though their sequence identities with the target are not high (29.9% for *E. coli* GlpF, 27.93% for human AQP1 and 27.46% for bovine AQP1). ProModII [25] was subsequently used to generate the model of the target using the templates. The generated comparative model of nodulin 26 comprises 215 residues from sequence numbers 36–250 which includes all six transmembrane helices and two half membrane-spanning helices of the monomer.

The model was then validated by PROCHECK. Short contacts and bad regions were rectified manually by InsightII (MSI, Inc.). All hydrogens were generated to fill the unoccupied valences of heavy atoms at the neutral state and the generated H atom positions were optimized by the BUILDER and DISCOVER3 modules of InsightII respectively. The molecule was then minimized, keeping all CA atoms fixed.

2.3. Docking of ligand molecules

Two formamide molecules, generated and optimized by the BUILDER module, were fitted at two regions of the nodulin 26 channel, one at the selectivity filter and one at the constriction region in a manner similar to glycerol binding in the GlpF channel [10]. The nodulin 26 complexed with two formamide molecules was solvated by 10 Å water layer by the SOAK utility of InsightII and the resulting system was then minimized by DISCOVER3 initially by steepest descent (SD) and then by conjugant gradient (CG) keeping all CA atoms fixed.

2.4. Tetramerization of nodulin 26

All the water molecules except those in the channel were removed from the structure and the tetramer assembly was generated using the same matrix having four-fold symmetry as used in the GlpF tetramer structure generation [10]. This tetramer assembly was then minimized by SD for 500 iteration steps keeping the CA atoms fixed. The structure was then analyzed by CONTACT implemented in CCP4 suite [26] of programs and no significant overlapping was found between the constituent monomers.

2.5. Membrane embedding and solvation of the nodulin 26 tetramer

A pre-equilibrated rectangular membrane bilayer of 340 (16:O/18:1C9) palmitoyloleyl phosphatidyl-ethanolamine (POPE) and 6628 water molecules was downloaded from the server http://moose.bio.ucalgary.ca. The membrane plane was parallel to the XY plane and the Z axis was perpendicular to the membrane plane. The tetrameric protein was placed at the center of the membrane box by optimal matching of hydrophobic surfaces of the protein with the hydrophobic mid part of the membrane bilayer and hydrophilic residues with hydrophilic head of the POPE bilayer. The channel axis was kept approximately parallel to the Z axis, i.e. perpendicular to the membrane plane. After placing the tetramer, the polar head and two aliphatic tails of the lipid molecules simultaneously clashing with the protein atoms were removed manually. But the lipids which had very few overlaps with protruding protein residues, either with their tail ends or polar head were kept to avoid generation of any void space in between the lipid bilayer and protein, expecting that the overlaps would be removed by minimization. A 5 Å water layer was generated by the SOAK utility of InsightII covering the entire system and their positions with respect to protein and lipid molecules were optimized. The resulting system with four protein chains of 215 amino acids each, eight formamide molecules, 185 POPE molecules and 1053 water molecules (a total of 62 985 atoms) were then subjected to molecular mechanics calculations (Fig. 2).

2.6. Molecular mechanics calculations

The system was minimized initially keeping protein and formamide molecules fixed for a few cycles using SD minimization to relax the lipid molecules and then rigorous minimization was performed keeping only CA atoms fixed. CONTACT (of CCP4 suite) [26] run on this system showed no significant overlapping between lipid and protein side chains. The minimized system was equilibrated for a short period of 10 ps keeping the protein part fixed which allowed the POPE bilayer to be accommodated around the protein molecules. Then the entire system was minimized for 300 iteration steps CG (down to a gradient < 10 kcal/mol/Å) without any constraint. This system was then equilibrated for a period of 210 ps with constant volume and temperature (NVT ensemble) through the velocity verlet integrator [27]. The temperature was kept at 310 K (physiological temperature and above gel–liquid crystalline phase transition temperature of POPE). The time step for integration was 2 fs using the RATTLE algorithm, a velocity version of SHAKE [28] with a tolerance of 1e-5 to constrain the bonds during simulation. The last 120 ps trajectory were analyzed saving the coordinates at every 0.2 ps interval. All the simulations were carried out with the CVFF forcefield and for non-bonded calculations, the cell multipole method along with a dielectric constant of 1 was used. The structure was finally analyzed for quality with PROCHECK.

2.7. Ligand binding studies

Since the binding of a ligand in the channel is specific in the region between the selectivity filter and the constriction region, five positions of the ligand were trapped from the four monomers during the last 120 ps trajectory in this region of the channel, one position at selectivity filter, two positions in between the selectivity filter and the constriction region, one at constriction region and at just after constriction region. These five positions of the ligand molecule were selected based on the following three criteria: (i) the duration of occupancy of the ligand molecule in those positions was ~ 10 ps in the trajectory, (ii) the positions of center of mass of the ligand molecule are distributed along 10 Å region of the channel axis between the selectivity filter and the constriction region near the –NPA– motif, and (iii) the interactions of the ligand molecule with the protein atoms in the channel are different in each of the five cases. Possible interactions of the ligand molecules with the protein channel in this region were analyzed by Ligplot [29].

3. Results and discussion

3.1. Overall fold

The transmembrane helical regions of nodulin 26 model structure adopt similar conformation to mammalian AQP1 and *E. coli* GlpF structure, the templates of the model, but all extracellular loops are shorter compared to them. The rms

```
sp|P29972|AQP1_HUMAN          VGHISGAHLNPAVTLGLLLSCQISIFRALMYIIAQCVGAIVATAILSGIT 116
sp|P55087|AQP4_HUMAN          FGHISGGHINPAVTVAMVCTRKISIAKSVFYIAAQCLGAIIGAGILYLVT 137
sp|P41181|AQP2_HUMAN          LGHISGAHINPAVTVACLVGCHVSVLRAAFYVAAQLLGAVAGAALLHEIT 108
sp|Q9WTY4|AQP5_MOUSE          LGPVSGGHINPAITLALLIGNQISLLRAIFYVAAQLVGAIAGAGILYWLA 109
sp|Q13520|AQP6_HUMAN          TWKTSGAHANPAVTLAFLVGSHISLPRAVAYVAAQLVGATVGAALLYGVM 122
sp|P08995|NO26_SOYBN          VGHISGGHFNPAVTIAFASTRRFPLIQVPAYVVAQLLGSILASGTLRLLF 137
tr|Q9XGG7|NLM_GARDENPEA       LGHISGAHFNPAVTIAFATTRRFPLKQVPAYIAAQVFGSTLASGTLRLLF 138
tr|O48595|NLM_ARABIDOPSIS     LGHISGAHINPAVTIAFASCGRFPLKQVPAYVISQVIGSTLAAATLRLLF 137
sp|Q92482|AQP3_HUMAN          AGQVSGAHLNPAVTFAMCFLAREPWIKLPIYTLAQTLGAFLGAGIVFGLY 123
sp|O14520|AQP7_HUMAN          AGRISGAHMNAAVTFANCALGRVPWRKFPVYVLGQFLGSFLAAATIYSLF 134
sp|P11244|GLPF_ECOLI          TAGVSGAHLNPAVTIALWLFACFDKRKVIPFIVSQVAGAFCAAALVYGLY 108
tr|Q8Z2Y7|GLPF_SALMONELLA    TAGVSGAHLNPAVTIALWLFACFDKRKVVPFIISQVAGAFCAAALVYGLY 108
                                  **.* *.*:*..          :   :  .*  *:  .:. :  :

sp|P29972|AQP1_HUMAN          LVLCVLATTDRRRRDL-GGSAPLAIGLSVALGHLLAIDYTGCGINPARSF 197
sp|P55087|AQP4_HUMAN          LVFTIFASCDSKRTDV-TGSIALAIGFSVAIGHLFAINYTGASMNPARSF 218
sp|P41181|AQP2_HUMAN          LVLCIFASTDERRGEN-PGTPALSIGFSVALGHLLGIHYTGCSMNPARSL 189
sp|Q9WTY4|AQP5_MOUSE          LALCIFSSTDSRRTSP-VGSPALSIGLSVTLGHLVGIYFTGCSMNPARSF 190
sp|Q13520|AQP6_HUMAN          LVLCVFASTDSRQTS---GSPATMIGISWALGHLIGILFTGCSMNPARSF 201
sp|P08995|NO26_SOYBN          LMFVICG-VATDNRAV-GEFAGIAIGSTLLLNVIIGGPVTGASMNPARSL 214
tr|Q9XGG7|NLM_GARDENPEA       LMFIISG-VATDNRAI-GELAGIAVGSTVLLNVMFAGPITGASMNPARSI 215
tr|O48595|NLM_ARABIDOPSIS     LMFIISG-VATDNRAI-GELAGLAIGSTVLLNVLIAAPVSSASMNPGRSL 221
sp|Q92482|AQP3_HUMAN          LIVCVLAIVDPYNNPVPRGLEAFTVGLVVLVIGTSMGFNSGYAVNPARDF 220
sp|O14520|AQP7_HUMAN          LQLCLFAITDQENNPALPGTEALVIGILVVIIGVSLGMNTGYAINPSRDL 231
sp|P11244|GLPF_ECOLI          LMGLILALTDDGNGVPRGPLAPLLIGLLIAVIGASMGPLTGFAMNPARDF 208
tr|Q8Z2Y7|GLPF_SALMONELLA    LMGLILALTDDGNGVPRGPLAPLLIGLLIAVIGASMGPLTGFAMNPARDF 208
*   : .     .           :*    :         :. .:**.*.:
```

Fig. 1. Some important portions of sequence alignment of AQP family of proteins by CLUSTAL W. The –NPA– motifs are shaded.

deviation values of all Cα atoms of nodulin 26 with AQP1 and GlpF are 2.61 and 3.33 Å respectively.

3.2. Selectivity filter

The selectivity filter region of the channel is amphipathic in nature like GlpF [10]. The hydrophilic part is contributed by Arg212 and Ser207 whereas the hydrophobic contributions are mainly coming from Trp77 and Val197 (Fig. 3a). Presence of Ser207 makes the binding of the ligand in a different manner compared to AQP1 and GlpF having Gly and Ala in this position respectively. Ser207OG interacts with the ligand in the region between the selectivity filter and the –NPA– constriction region (Fig. 3a–c).

3.3. Probable ligand binding

The binding of the ligand is highly specific for the region from the selectivity filter to the constriction region along the channel and mediated mainly by side chain atoms whereas the binding at the other regions of the channel is mediated by the backbone oxygens. Biochemical studies indicate that the nodulin 26 of soybean root nodule SM has the highest permeability towards formamide [17]. Our model structure demonstrates the mode of formamide binding in the lumen of nodulin 26. At the selectivity filter, the binding of formamide is mediated through hydrogen bonds between Ser207OG–NH2 and Arg212NH1–O, whereas the CH atom of the formamide molecule faces a hydrophobic region formed by Val197 and Trp77 (Fig. 3a).

In the region between the constriction region and the selectivity filter, the ligand mainly interacts with the OG and backbone O atoms of Ser207 and with Asn209 of the –NPA– motif from C-terminal half. The hydrophobic interactions are provided by the Leu50 side chain atoms (Fig. 3b,c).

At the constriction region, the formamide molecule interacts with Asn97 by strong H bonds with their opposite polarity atoms (Fig. 3d), the hydrophobic interactions here are provided by the Leu193 side chain atoms.

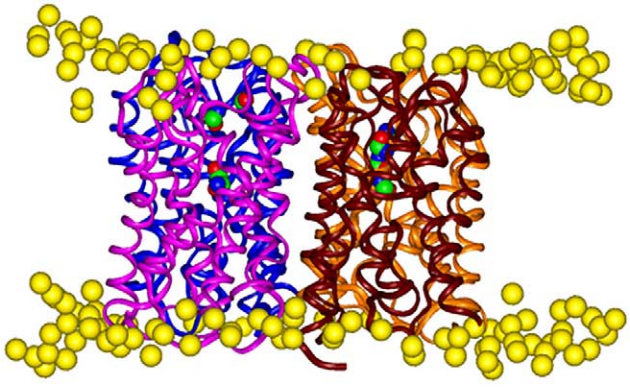

Fig. 2. Tetramer assembly of nodulin 26; monomers are represented in different colored ribbons. The phosphate heads of the POPE bilayer molecules are only displayed and represented by yellow balls. The formamide molecules in the channels are represented in CPK model. (For interpretation of the references to colour in this figure legend, the reader is referred to the web version of this article.)

3.4. Comparison with AQP1 and GlpF

Though the overall structure of nodulin 26 is closely related to AQP1 and GlpF, some important differences are observed in nodulin 26 compared to other members of this class of proteins. Ser207 at the selectivity filter of nodulin 26 is only conserved in the NIP and TIP subfamilies. Residue in the equivalent position is glycine in AQP1 [9] and alanine in GlpF [10] though serine is also found in AQP2, AQP4 and AQP5. The role of serine side chain in ligand binding and the channel transport mechanism is not yet established from the known structures [9,10]. Homology modeling of nodulin 26 and ligand binding studies indicate an important role of Ser207. The hydrophilic contribution at the selectivity filter mainly comes from the arginine residue of Ar/R motif (aro-

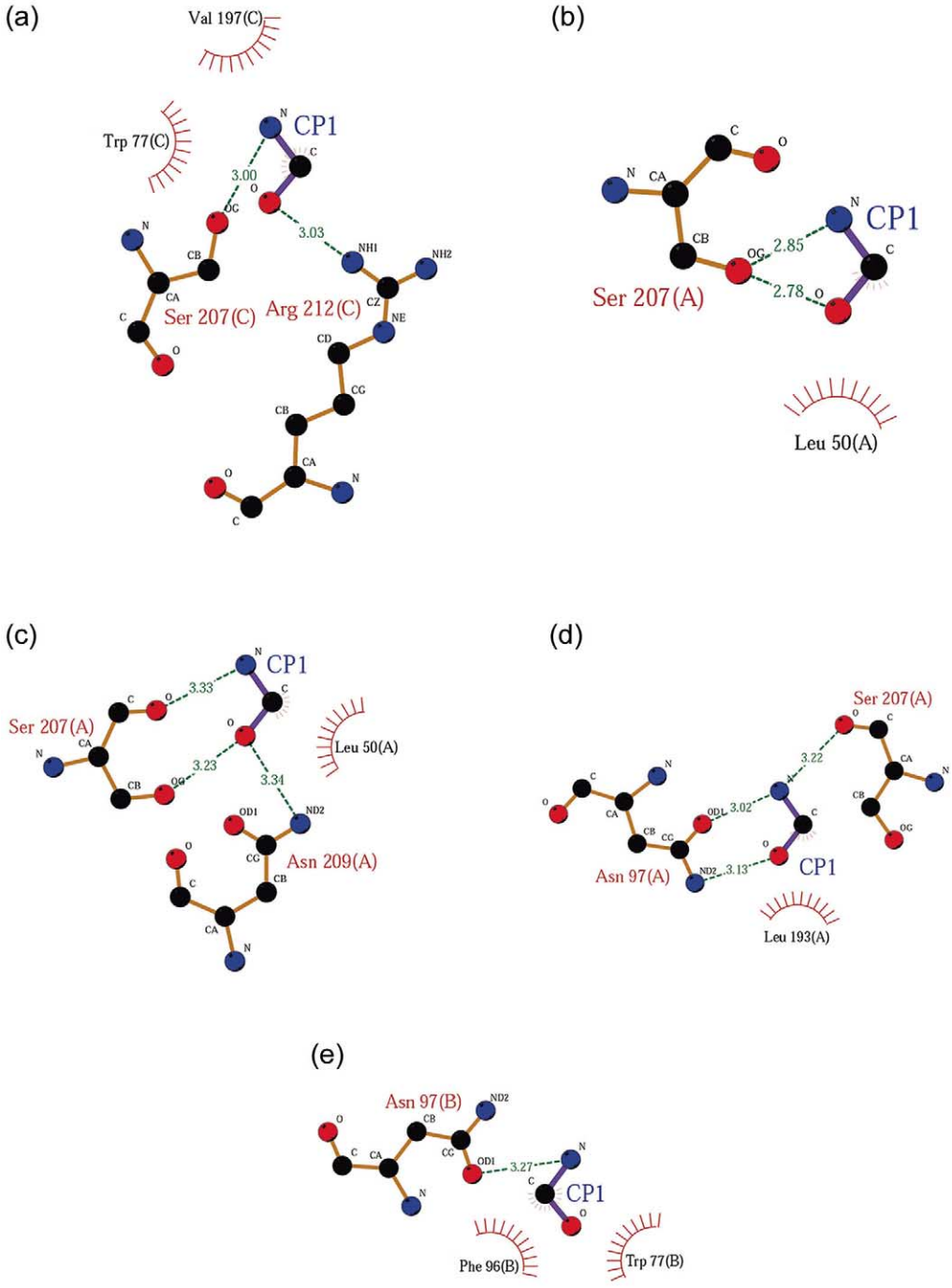

Fig. 3. Ligplot [29] of formamide molecule (CP1) at different parts of the channel: a: at the selectivity filter, b, c: in between the selectivity filter and the constriction region, d: at the constriction region, and e: just after passing the constriction region. H bondings are indicated by green dots and hydrophobic interactions are indicated by radial lines around atoms or residues. (For interpretation of the references to colour in this figure legend, the reader is referred to the web version of this article.)

Table 1
Φ and Ψ angles of the residues of the –NPA– motif (P4, P5, P6) near the cytoplasmic side and three preceding residues (P1, P2, P3) of nodulin 26, AQP1 [9] and GlpF [10]

Protein	P1	Φ	Ψ	P2	Φ	Ψ	P3	Φ	Ψ	Asn (P4)		Pro (P5)		Ala (P6)	
										Φ	Ψ	Φ	Ψ	Φ	Ψ
GlpF	Ala	51.9	−115.0	His	−77.8	121.8	Leu	51.5	−153.5	−165.8	−62.1	−55.16	142.6	−65.2	143.3
AQP1	Ala	48.3	−126.8	His	−68.4	117.6	Leu	53.9	−155.4	−170.2	−68.7	−47.4	143.0	−64.0	148.5
Nodulin 26	Gly	−153.6	−94.1	His	−119.8	57.7	Phe	−160.4	155.9	−114.7	−75.0	−40.0	130.7	−72.4	113.5

matic/arginine) for AQP1 and GlpF [9,10]. In nodulin 26, this hydrophilic contribution comes from both Arg212 as well as Ser207. The interactions of Ser207OG with the ligand are extended even when the ligand crosses the selectivity filter and enters the region of the channel between the selectivity filter and the constriction region. In this case, another rotamer of Ser207 side chain interacts with the ligand. During 120 ps trajectory, a transition of χ_1 value for Ser207 is observed indicating the two rotamers (Fig. 4b). When the ligand is at the constriction region, the Ser207OG again moves to the

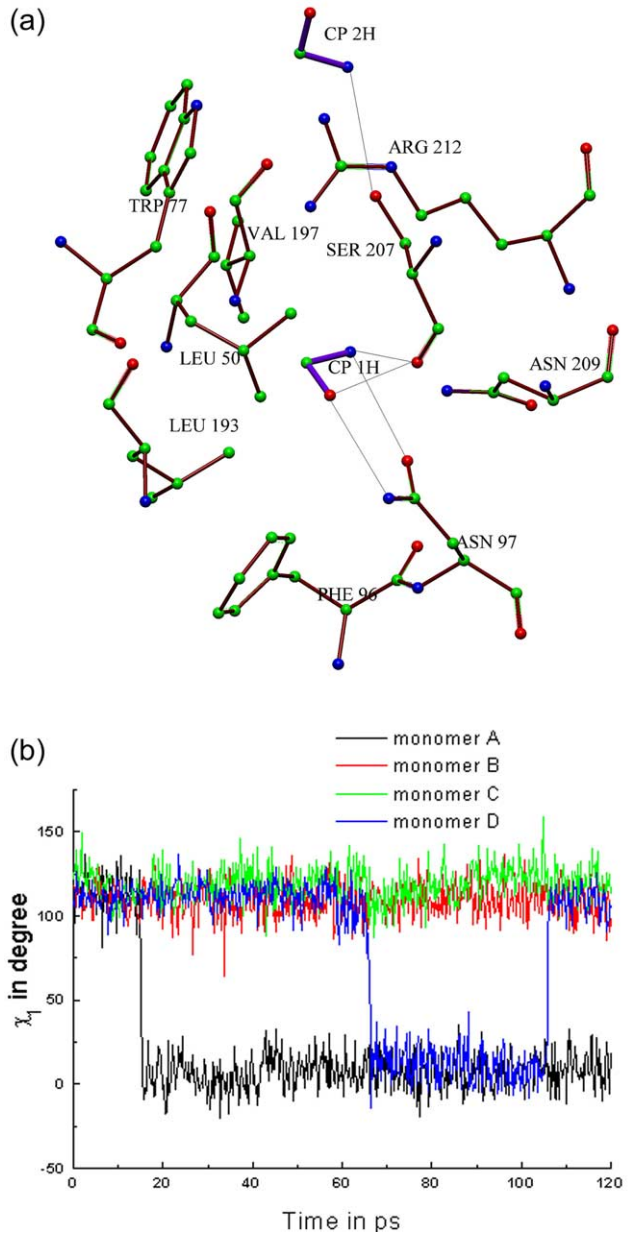

Fig. 4. a: Interaction of second formamide molecule (CP2) with Ser207 when the first one (CP1) reaches at the constriction region. b: Two rotamer conformations, indicated by side chain torsion angle χ value of Ser207 during the 120 ps trajectory for four monomers A, B, C and D. Ser207 in monomers A and D changes their side chain conformation in the trajectory. χ_1 value near zero corresponds to the conformation of Ser207 when it interacts to ligand molecule at the region in between the selectivity filter and the constriction region.

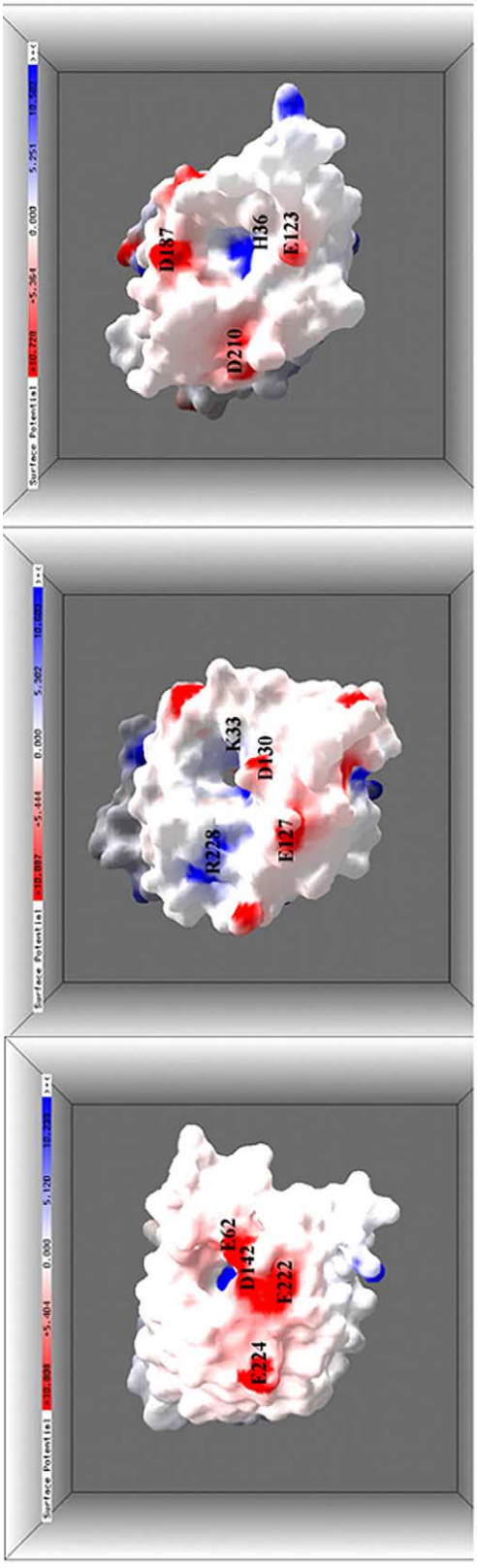

Fig. 5. Comparison of electrostatic potential surfaces of nodulin 26, GlpF and AQP1 at the extracellular face. The figure was generated by GRASP [30].

previous orientation and interacts with a second ligand (Fig. 4a).

Another important difference is found near the cytoplasmic side of the channel of nodulin 26 from that of AQP1 and GlpF. The transport of ligand is mediated by three backbone carbonyl oxygens in the loop region just before the start of the –NPA– motif in this region as revealed in the known structures [15]. Previous MD simulations on AQP1 and GlpF [11,14] indicated that this loop has both functional and positional relevance. The loop mobility and pore diameter in this region of the channel is partly contributed by a pair Phe24–Leu149 in AQP1 and Leu21–Leu159 in GlpF [12]. Phe24 in AQP1 intrudes more into the pore [15] and significantly influences the size of constriction. In the nodulin 26 model structure though there is a Leu50–Leu167 pair at the equivalent position, the size of the channel is constricted by Phe96, a residue preceding the –NPA– motif near the cytoplasmic side. A Phe residue in this position is found and conserved in the NIP family only, while the other families have smaller hydrophobic residues like Leu (in AQP1 and GlpF), Ile, Ala, etc. This Phe96 makes a stacking interaction with His95 and the His95ND1 is hydrogen bonded to Thr101OG1, both the interactions being consistent in the trajectory. These interactions together with the presence of a bulky side chain of Phe96 increase the rigidity in this region of the loop of nodulin 26 and change the loop's backbone conformation from that of AQP1 and GlpF while the backbone conformation of the –NPA– motif is almost similar (Table 1). So a different ligand binding and transport mechanism is expected for the NIP family members in this region of the channel.

The extracellular loops in nodulin 26 are shorter compared to AQP1 and GlpF. A broader opening of the channel at the extracellular space is observed in the case of nodulin 26. Electrostatic surface potential of nodulin 26 is quite different from AQP1 and GlpF. An abundance of electronegative charge is observed in nodulin 26 (Fig. 5) near the channel opening at the extracellular space.

4. Conclusion

Overall structure of nodulin 26 is similar to AQP1 and GlpF with shorter extracellular loops that cause a broader opening of the channel. The electrostatic potential surface calculation indicates a highly electronegative surface at the extracellular region of the channel. Presence of a serine residue at the selectivity filter and a phenylalanine, which precedes the –NPA– motif near the cytoplasmic side, indicate a different ligand binding and transport mechanism for NIP class of proteins.

Acknowledgements: I thank Prof. J.K. Dattagupta, Prof. C. Chakrabarti, Dr. U. Sen and Ms. J. Dasgupta of our Institute for their valuable discussion and critical comments on this work. I also thank Mr. A. Bhattacharyya for help in preparing the figures in the manuscript.

References

[1] Schrier, R.W. and Cadnapaphornchai, M.A. (2003) Prog. Biophys. Mol. Biol. 81, 117–131.
[2] Thomas, D., Bron, P., Ranchy, G., Duchesne, L., Cavalier, A., Rolland, J., Raguenes-Nicol, C., Hubert, J., Haase, W. and Delamarche, C. (2002) Biochim. Biophys. Acta 1555, 181–186.
[3] Santonov, V.S., Javot, H. and Maurel, C. (2000) Curr. Opin. Plant Biol. 3, 476–481.
[4] Maurel, C. and Chrispeels, M.J. (2001) Plant Physiol. 125, 135–138.
[5] Johanson, U., Karlsson, M., Johanson, I., Gustavsson, S., Sjoval, S., Fraysse, L., Weig, A.R. and Kjellbom, P. (2001) Plant Physiol. 126, 1358–1369.
[6] Chaumont, F., Barrieu, F., Wojcik, E., Chrispeels, M.J. and Jung, R. (2001) Plant Physiol. 125, 1206–1215.
[7] Johanson, U. and Gustavsson, S. (2002) Mol. Biol. Evol. 19, 456–461.
[8] Nollert, P., Harries, W.E.C., Fu, D., Miercke, L.J.W. and Stroud, R.M. (2001) FEBS Lett. 504, 112–117.
[9] Sui, H., Han, B., Lee, J.K., Walian, P. and Jap, B.K. (2001) Nature 414, 871–878.
[10] Fu, D., Libson, A., Miercke, L.J.W., Weitzman, C., Nollert, P., Krucinski, J. and Stroud, R.M. (2000) Science 290, 481–486.
[11] Zhu, F., Tajkhorshid, E. and Schulten, K. (2001) FEBS Lett. 505, 212–218.
[12] Fujiyoshi, Y., Mitsuoka, K., Groot, B.L., Philippsen, A., Grubmuller, H., Agre, P. and Engel, A. (2002) Curr. Opin. Struct. Biol. 12, 509–515.
[13] Tajkhorshid, E., Nollert, P., Jensen, M., Miercke, L.J.W., O'Connell, J., Stroud, R.M. and Schulten, K. (2002) Science 296, 525–530.
[14] Jensen, M., Tajkhorshid, E. and Schulten, K. (2001) Structure 9, 1083–1093.
[15] Groot, B.L. and Grubmuller, H. (2001) Science 294, 2353–2356.
[16] Zardoya, R. and Villalba, S. (2001) J. Mol. Evol. 52, 391–404.
[17] Rivers, R.L., Dean, R.N., Chandy, G., Hall, J.E., Roberts, D.M. and Zeidel, M.L. (1997) J. Biol. Chem. 272, 16256–16261.
[18] Niemietz, C.M. and Tyerman, S.D. (2000) FEBS Lett. 465, 110–114.
[19] Lee, J.W., Zhang, Y., Weaver, C.D., Shomer, N.H., Louis, C.F. and Roberts, D.M. (1995) J. Biol. Chem. 270, 27051–27057.
[20] Klebl, F., Wolf, M. and Sauer, N. (2003) FEBS Lett. 547, 69–74.
[21] Wallace, I.S., Wills, D.M., Guenther, J.M. and Roberts, D.M. (2002) FEBS Lett. 523, 109–112.
[22] Roberts, M.D., Rivers, R.L., Zeidel, M.L. and Roberts, D.M. (1999) Biochemistry 38, 347–353.
[23] Schwede, T., Kopp, J., Guex, N. and Peitsch, M.C. (2003) Nucleic Acids Res. 31, 3381–3385.
[24] Bernstein, F.C., Koetzle, T.F., Williams, G.J.B., Meyer, E.F., Brice, M.D., Rodger, J.R., Kennard, O., Shimanouchi, T. and Tasumi, M. (1977) J. Mol. Biol. 112, 535–542.
[25] Peitsch, M.C. (1996) Biochem. Soc. Trans. 24, 274–279.
[26] Collaborative Computational Project, Number 4 (1994) Acta Cryst. D 50, 760–763.
[27] Verlet, L. (1967) Phys. Rev. 159, 98–103.
[28] Ryckaert, J.P., Ciccotti, G. and Berendsen, H.J.C. (1977) J. Comp. Phys. 23, 327–331.
[29] Wallace, A.C., Laskowski, R.A. and Thornton, J.M. (1995) Protein Eng. 8, 127–134.
[30] Nicholls, A., Sharp, K. and Honig, B. (1991) Proteins SFG 11, 281–296.